DESIGN FOR ADDITIVE MANUFACTURING: INTEGRATING STRUCTURAL OPTIMIZATION AND PRINTABILITY ANALYSIS FOR AEROSPACE COMPONENTS

Bianca Omede'
Department of Aerospace Science and Technology, Politecnico di Milano
Milan, Italy

Simone Festa
Department of Aerospace Science and Technology, Politecnico di Milano
Milan, Italy

Maurizio Tirelli
Leonardo S.p.A.
Cascina Costa (VA), Italy

Gabriele Fantoni
Leonardo S.p.A.
Cascina Costa (VA), Italy

Sergio Sartori
Leonardo S.p.A.
Cascina Costa (VA), Italy

Antonio Mattia Grande
Department of Aerospace Science and Technology, Politecnico di Milano
Milan, Italy

ABSTRACT

Aeronautical components are increasingly being used in aerospace applications, demonstrating the importance of balancing structural optimization and manufacturability in order to meet demanding performance and certification standards. In this study, a well-established aerospace component was analyzed and redesigned to exploit the advantages of additive manufacturing through a comprehensive workflow combining finite element analysis, topology optimization, and printability assessment. The methodology aims to bridge the gap between the advanced research developed in industry and Universities and the practical production readiness of AM parts, enabling a more holistic design workflow that considers not only structural performance but also the constraints associated with the additive process. Specifically, the study focuses on the integration of printability and build orientation analyses as coupled processes within the optimization workflow, enabling a truly printability-driven design for additive manufacturing from the earliest stages of component development. In particular, the methodology is applied to the redesign of a metallic aeronautical bracket developed by Leonardo Helicopters, which is currently manufactured using conventional methods and installed on a helicopter. The proposed methodology demonstrates the potential for accelerating DfAM workflows in an industrial context, reducing the time between design and production and ensuring geometric and functional conformity of critical flight components manufactured using metal AM.

NOTATION

*

Symbols

$R_{a,\mathrm{lim}}$ Acceptable surface roughness threshold, μm

F_i Component of the force vector in the i-th direction

$\rho_{\mathrm{component}}$ Component relative density, %

L_{warp} Critical warping length, mm

Ω Design domain

$\mathbf{u}$ Displacement field

ε_{b} Elongation at break, %

C_0 Elasticity tensor of solid material

$\mathbf{F}$ External force vector

$\mathbf{K}(\rho)$ Global stiffness matrix

V_0 Initial design domain volume, mm^3

V_{build} Maximum build volume, mm^3

$\theta_{\max}$ Maximum overhang angle, °

$C(\rho)$ Penalized elasticity tensor

$E(\rho)$ Penalized Young's modulus

p Penalization exponent

ν Poisson's ratio, -

C_{powder} Powder cost, $/kg

ρ_{powder} Powder density, g/cm^3

$\rho(x)$ Pseudo-density function

$\varepsilon(\rho)$ Strain field

$V_{\textbf{target}}$ Target volume fraction

t_{thin} Thin wall detection threshold, mm

$U(\rho)$ Total strain energy

σ_{UTS} Ultimate tensile strength, MPa

σ_{y} Yield strength, MPa

E_0 Young's modulus of solid material

E Young's modulus, GPa

*

Acronyms

AM Additive Manufacturing

CAD Computer-Aided Design

CAE Computer-Aided Engineering

CPU Central Processing Unit

DfAM Design for Additive Manufacturing

FE Finite Element

FEM Finite Element Method

LPBF Laser Powder Bed Fusion

NGCTR Next Generation Civil Tilt-Rotor

Ra Arithmetic Mean Roughness

SIMP Solid Isotropic Material with Penalization

SLM Selective Laser Melting

STL Stereolithography File Format

TO Topology Optimization

UTS Ultimate Tensile Strength

INTRODUCTION

In recent years, Additive Manufacturing (AM) has redefined the boundaries of product development. It enables the production of geometrically complex components that were previously impossible to realize using conventional manufacturing methods (Refs. 1, 2). However, leveraging these unprecedented possibilities requires a change in design philosophy, which is embodied by the concept of Design for Additive Manufacturing (DfAM) (Refs. 3, 4).

DfAM aims to tailor the geometries of parts to the unique constraints and possibilities of AM processes. This enables part consolidation, weight reduction, performance enhancement and process simplification, providing a comprehensive framework for harnessing the full potential of AM technologies to drive engineering innovation. Building on the traditional principles of design for manufacturing and assembly, DfAM works on several levels: adapting geometries to AM constraints, evaluating their impact on manufacturing quality and linking design decisions to production outcomes (Ref. 4). Over the last decade, a variety of approaches have emerged, from practical design heuristics to formal frameworks that aim to integrate DfAM principles in the early stages of product development (Refs. 5–7).

These strategies have fallen on fertile ground in the aerospace industry in particular (Ref. 8), and more recently in rotorcraft applications, where the demand for lightweight, high-performance components is crucial. In the helicopter industry, additive manufacturing has been used to redesign and manufacture parts such as auxiliary lubrication tanks, pump housings and gearbox components, enabling significant weight savings and geometric flexibility. For example, Leonardo Helicopters has developed and tested additively manufactured components for the input module of the Next Generation Civil Tilt-Rotor (NGCTR) demonstrator, including a topologically optimized auxiliary oil tank manufactured from AlSi10Mg using Selective Laser Melting (SLM). The design enabled efficient use of space, improved vibration performance and weight reduction while ensuring structural integrity under dynamic loads (Ref. 9). Similarly, Airbus Helicopters has invested in a dedicated 3D printing center at its Donauwörth site, where titanium and aluminum parts are produced for both prototypes and series production. This includes components for experimental platforms such as the CityAirbus NextGen and the Racer high-speed demonstrator, where AM enables rapid iteration and integration of complex geometries (Ref. 10).

Such applications illustrate the increasing importance of DfAM in rotorcraft design, where the integration of structural optimization and manufacturability is crucial to meet demanding performance and certification standards. In this context, DfAM is not just a design philosophy, but a strategic enabler for the next generation of rotorcraft and aircraft development, contributing to sustainability goals, reducing buy-to-fly rates and accelerating prototyping and customization of mission-critical components (Refs. 11, 12). As additive manufacturing evolves from a prototyping technique to a certified production method in highly regulated industries such as aerospace, the demand for integrated design approaches that balance mechanical performance and printability is becoming increasingly important. At the same time, a key barrier to widespread adoption is the lack of expertise and the need for specialized tools, design rules and methods to support reliable and efficient implementation.

One of the most powerful tools for exploiting the design freedom offered by AM is Topology Optimization (TO), an approach that identifies the optimal material distribution within a design domain for a given set of loads and constraints (Ref. 13). Topology-optimized structures can achieve a high degree of structural efficiency while reducing weight, which is of paramount importance in performance-relevant industries such as aerospace (Ref. 14). Nevertheless, it is not trivial to transfer these optimized geometries directly into manufacturable parts. Irregular shapes can require extensive support structures or lead to build failures due to warping, overheating or anisotropic behavior during the printing process (Refs. 2, 15).

Currently, most studies on the application of TO focus on the design of aerospace structural aerospace components concentrate on brackets, due to their relatively simple boundary conditions and their high potential for weight reduction. Numerous works successfully demonstrate the integration of TO into the workflows of additive manufacturing of metal parts for such components. For example, Ferreira et al. (Ref. 16) applied a combined topology and shape optimization method supported by finite element modeling to redesign a bracket produced with laser-based AM. Their approach resulted in a geometry that reduced weight while ensuring structural compliance under real-world loading conditions, showcasing the potential for a realistic integration of structural optimization and process-aware simulation workflows. Similarly, Satya Hanush and Manjaiah (Ref. 14) optimized a structural bracket component using TO tailored to AM constraints. The redesigned component exhibited a better strength-to-weight ratio with special attention paid to material deposition paths and build orientation, demonstrating the importance of balancing optimization results with manufacturing feasibility. Seabra et al. (Ref. 17) investigated the use of SLM to produce topology-optimized brackets and emphasised the benefits of weight reduction without compromising structural integrity. Their case study showed that design strategies based on topology optimization not only reduce the overall mass, but also minimize the number of support structures required during manufacturing.

This has led to a growing body of research that focuses on combining structural optimization and printability analysis to develop integrated design methods that not only maximize performance but also ensure manufacturability. This coupling is particularly important in the aerospace industry, where stringent certification standards go hand in hand with the demand for lighter, structurally optimized and cost-effective parts (Refs. 11, 12).

In this context, special attention has been paid to the optimization of build orientation, as this has a direct impact on critical aspects of printability, such as surface quality, dimensional accuracy, anisotropy, support requirements and thermally induced distortion. Several methods have been proposed to overcome this multi-objective challenge. For example, Zwier and Wits (Ref. 18) presented a feature-based approach that uses convex hulls and ray-tracing analyses to reduce overhangs and support structures, while Cheng and To (Ref. 19) presented a Pareto-based evolutionary algorithm capable of balancing build time, surface finish and volume of support material based on a weighted target. Budinoff and McMains (Ref. 20) developed a manufacturability assessment toolbox that combines a few geometric features with orientation-sensitive AM constraints to provide early design feedback. In the meantime, Sheng et al. (Ref. 21) proposed a comprehensive multi-criteria decision-making framework that considers surface orientation, support minimization, and structural risks, highlighting the increasing complexity of integrating manufacturability into automated decision-making workflows.

Despite these advances, many approaches still struggle to incorporate structural performance and real-world constraints into orientation optimization strategies. With the transition from AM to production-ready applications in highly regulated sectors, the development of an integrated design workflow that considers topology optimization, printability analysis and build orientation simultaneously is a crucial step towards reliable and certifiable part production. A knowledge-based engineering framework has been proposed to automate non-creative tasks and support multidisciplinary design optimization in DfAM (Ref. 7). In this context, it is crucial to prioritize the automation of design iterations after the initial phase. By automating these traditionally manual steps, the design workflow can be accelerated, human involvement reduced and manufacturability optimized from the outset, ensuring that design modifications are consistently refined according to predefined constraints and objectives.

In this context, DfAM is evolving from a set of guidelines to an integrated, data-driven paradigm, that combines structural analysis, AM process constraints and downstream considerations such as part orientation, support minimization and thermal distortion control. The present work contributes to this evolving landscape by proposing a structured framework for the design and manufacturability assessment of aerospace components for additive manufacturing. The proposed methodology aims to bridge the gap between the advanced research developed in industry and Universities and the practical production readiness of AM parts. In particular, the study focuses on the integration of topology optimization and printability analysis to enable a more holistic design workflow that considers not only structural performance but also the constraints associated with the additive process.

By combining simulation-driven design and printability-aware evaluation, this work demonstrates the potential for accelerating DfAM workflows in an industrial context, reducing the time between design and production and ensuring geometric and functional conformity of critical flight components manufactured using metal AM. As a case study, the methodology is applied to the redesign of a metallic aeronautical bracket developed by Leonardo Helicopters, which is currently manufactured using conventional methods and installed in the rear section of a helicopter. The component is subjected to typical loading conditions representative of its operational environment. The design process includes the formulation of boundary conditions, material selection, topology optimization taking into account structural and mass constraints and a subsequent assessment of the component's printability, including overhang analysis, estimation of support and orientation sensitivity. This printability assessment is performed using *AM-Optimizer*, a custom MATLAB-based tool developed in-house to support automated orientation analysis and manufacturability evaluation of complex AM components (Ref. 22).

The article is structured as follows. The next section presents the materials and methods used in this study, including a detailed description of the constraints applied to the reference component selected for the redesign, the setup of the finite element model used to define the structural boundary conditions, the topology optimization strategy, an overview of the selected printable material, and the methodology underlying the application *AM-Optimizer* for printability evaluation. The results of the redesign are then presented, illustrating the evolution of the component at each design stage and comparing the final solution with the original configuration in terms of both structural performance and additive manufacturability. The final section concludes the study and outlines possible directions for future developments.

MATERIALS AND METHODS

A bracket is a structural component used to support and transfer loads within an assembly. In this context, the bracket acts as a load-bearing element that is primarily subjected to critical compressive forces, both static and cyclic. Its role is crucial for mechanical stability and load transfer between the connected parts. Therefore, understanding the loading conditions of the bracket and optimizing its geometry are essential steps, not primarily to achieve a lightweight design, but rather to enable a redesign that makes the part manufacturable by additive processes. The aim is to obtain a part that performs comparably to a traditionally machined counterpart while ensuring that its printability can be assessed in advance and that it meets the required technical specifications.

Due to confidentiality agreements with the company, all quantities reported in this work are normalized to prevent disclosure of proprietary information. For the same reason, the actual dimensions of the object cannot be disclosed.

Design constraints for the bracket

The bracket analyzed in this work is connected to the underlying structure by pins and collars, while a tie rod is attached to the holes provided in the bracket using socket head cap screws. For the purpose of finite element analysis, the former connections are simplified as constraints on the anchoring holes. In the latter case, kinematic coupling connections are used, enforcing equal displacements in all three directions and a rotational behavior defined by a reference point, thus replicating the effect of the bolt-based constraints with an efficient and controlled approximation.

The component is subjected to critical static compressive loads, which are given in Table 1 as a percentage of the maximum total load. Accurate knowledge of these critical static loads is essential for evaluating the structural response of the bracket and for guiding design decisions to ensure sufficient strength and stability in the static analysis.

Table 1. Static critical loads as percentage of the maximum total compression load.

Load direction	Static load [%]
F_x	0.83
F_y	84.7
F_z	14.47

Topology optimization

Most commercially available FEM programs that support TO use a density-based approach, namely the Solid Isotropic Material with Penalization (SIMP) interpolation method. Originally developed by Rozvany et al. (Ref. 23), the SIMP method is based on the fundamental approach introduced by Bendsøe and Sigmund (Ref. 13) and interpolates the material properties based on a pseudo-density variable $\rho(x) \in [0,1]$. Abaqus/CAE implements topology optimization using this SIMP approach with the aim of minimizing the strain energy of the structure and thereby maximizing the stiffness while satisfying the volume and design constraints. The SIMP method defines the modulus of elasticity $E(\rho)$ as a function of the pseudo-density:

$$E(\rho) = \rho^p E_0 \tag{1}$$

where E_0 is the modulus of elasticity of the solid material, ρ is the element density and $p > 1$ is the penalization factor (typically $p = 3$) used to discourage intermediate densities and steer the solution towards a binary material distribution (solid or void). The topology optimization problem is then formulated as follows:

$$\min_{\rho} U(\rho) = \frac{1}{2} \int_{\Omega} \varepsilon(\rho)^T C(\rho) \varepsilon(\rho) \, d\Omega \tag{2}$$

subject to the constraints:

$$\int_{\Omega} \rho(x) \, d\Omega \leq V_{\text{target}} \cdot V_0 \tag{3}$$

$$0 < \rho_{\min} \leq \rho(x) \leq 1 \quad \text{in } \Omega \tag{4}$$

Here $C(\rho) = \rho^p C_0$ is the elasticity tensor that depends on the penalized density, and ε is the strain field derived from the displacement solution of the finite element model. Abaqus/CAE solves this problem iteratively by updating the density distribution to reduce the strain energy while satisfying the constraints.

Material and printing technology

In the original design, the bracket component was made of Al7050 and produced by machining. However, as Al7050 is not suitable for additive manufacturing, it was necessary to find a substitute material. A printable aluminum alloy with comparable mechanical performance was identified in the literature: a high-strength Al-Cu-Mg alloy from the 2xxx series that is compatible with Laser Powder Bed Fusion (LPBF) technology (Ref. 24). Table 2 summarizes the mechanical and material properties of the selected Al2024-RAM2 (Al_2CuMg) alloy measured two months after printing in the as-built condition (Ref. 25). Moreover, the material appears to exhibit a fatigue strength of approximately 125 MPa at 10^6 cycles in the as-built condition, based on the available data and assuming a conservative estimate (Refs. 24, 26, 27). The data on surface roughness, also in the as-built condition, are shown in Table 3 at different build angles (Ref. 26). In addition to the material properties, several process-related parameters play a key role in evaluating the printability of the bracket using SLM-based LPBF technology. The reference values adopted in this study are summarized in Table 4, and include the powder density, powder cost, acceptable surface roughness limit, thin-wall detection threshold, critical warping length, maximum build volume, and maximum allowable overhang angle. The collected values are of course subject to a strong influence of printing parameters and subsequent surface treatments, but they serve as a guide to the properties and surface quality achievable with this material and this printing technology. Despite the benefits of additive manufacturing, critical features such as mounting holes must be post-processed to achieve precise tolerances required for screw-in and secure assembly. For this reason, the areas immediately adjacent to the holes are not considered in the FEM analysis as they are partially machined and the modeling of the bolted joint is simplified. However, these regions cannot be completely excluded from the simulation model, as it is necessary to extract the STL file of the complete part for the printing assessment.

Table 2. Material and mechanical properties of the as-built Al2024-RAM2 material measured two months after printing (Ref. 25).

Property	Symbol	Value
Young's modulus	E	75 GPa
Yield strength	σ_y	414 MPa
Ultimate Tensile Strength	σ_{UTS}	465 MPa
Elongation at break	ε_b	11 %
Poisson's ratio	ν	0.33
Component density	$\rho_{component}$	99.6 % (of ρ_{powder})

Table 3. Surface roughness (Ra) of as-built Al2024-RAM2 at different build angles, for a layer thickness of 30 μm (Ref. 26).

Build Angle [°]	Ra [μm]
0	4.95
20	7.41
90	4.79
160	9.22
180	5.61

Table 4. Key parameters of the LPBF process for Al2024-RAM2 used in the printability analysis. Values are indicative and subject to machine and setup specifications.[a]

Parameter	Symbol	Value
Powder density	ρ_{powder}	2.81 g/cm^3
Powder cost	C_{powder}	\$100 / kg
Acceptable Ra limit	$R_{a,lim}$	7 μm
Thin-wall detection threshold	t_{thin}	0.5 mm
Critical warping length	L_{warp}	60 mm
Maximum build volume	V_{build}	270 × 270 × 420 mm^3
Maximum overhang angle	θ_{max}	30°

[a] Values are taken from previously cited references (Refs. 24–27) and partly from previous experience with metal additive manufacturing at Leonardo S.p.A.

AM-Optimizer: an application for printability analysis

The printability analysis is performed with an internal application named *AM-Optimizer* (Ref. 22). This application has not yet been distributed and has only recently been developed, without being demonstrated on an industrial metal additive component. This application offers two important functions: the selection of the optimal build orientation and the analysis of printability for a given build angle. Specifically, the application optimizes the print orientation by performing a convex hull analysis of the part in STL format. Factors considered in determining the optimal orientation include the need for support structures, the risk of warping, the surface quality of the part, the base contact area, the height of the part and the presence of overhangs on thin walls. This approach to printability optimization has been shown to outperform traditional methods in terms of computational efficiency and adaptability to different additive manufacturing technologies. In addition, this application offers better customizability and greater transparency in selecting the optimal print orientation compared to commercial software. It allows for highly personalized optimization parameters ranging from printer specifications to a custom surface roughness model, enabling a tailored approach for each specific use case. These innovations significantly improve both the user-friendliness and competitiveness of the application. In addition, the application will be available free of charge, promoting wider accessibility and enabling use in different contexts. Figure 1 shows the graphical interface of the 'Orientation Optimization' section of the *AM-Optimizer* application as an example.

Furthermore, the application allows users to manually assign weights to the different components of the objective function used for orientation optimization, so that the same part can be evaluated according to the specific preferences and constraints of the chosen application scenario. Warping can lead to distortions and printing errors, while a larger base contact area improves adhesion and minimizes the risk of detachment during the printing process. The presence of overhangs on thin walls increases the likelihood of distortion and requires additional support, which in turn increases material consumption and post-processing time. Surface roughness also has a direct impact on the quality of the finished part and may require further post-processing steps. Additionally, the maximum height of the part along the selected build orientation is also taken into account, as it is directly proportional to the printing time and therefore plays an important role in production efficiency. By allowing the user to adjust the relative importance of these criteria, the application enables a print orientation strategy that is better suited to the specific requirements of the part, the additive manufacturing technology used and the planned application.

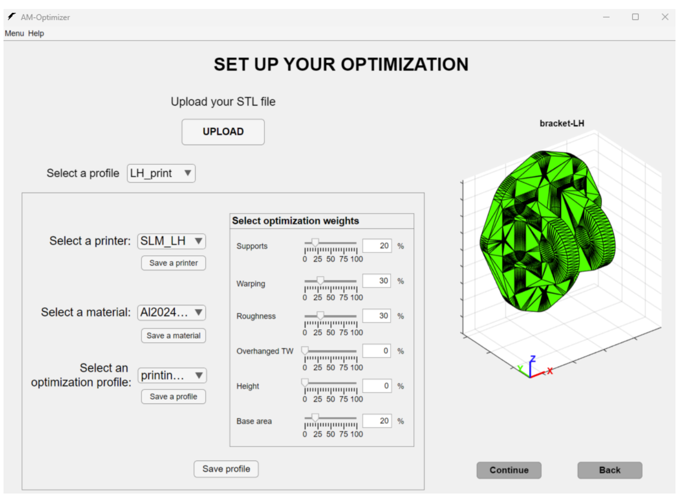

Figure 1. Orientation optimization interface of *AM-Optimizer*.

RESULTS AND DISCUSSION

Results before redesign for additive manufacturing

The part was meshed using quadratic tetrahedral elements (C3D10), and a mesh convergence study was performed to ensure the accuracy and reliability of the finite element results. Figure 2 shows the normalized stress distribution (with respect to the maximum value) obtained from the FEM analysis of the static load case of the bracket using Al2024-RAM2 material. Considering the great similarity of the elastic properties of Al2024-RAM2 and Al7050, and considering that the analysis is carried out entirely in the elastic range, the results obtained with Al2024-RAM2 are practically indistinguishable from those obtained with Al7050. Accordingly, both the location of the maximum stress concentrations and the qualitative distribution of stresses, including those resulting from the fatigue analysis, are practically identical in both cases. Since the two materials have comparable fatigue limits for the target service life, there are no significant differences in terms of fatigue performance. At this stage of the analysis, the only notable deviation concerns mass, which is due to the slightly higher density of Al2024-RAM2. Taking the mass of the original Al7050 component as 1, the corresponding mass for Al2024-RAM2 is 1.0416.

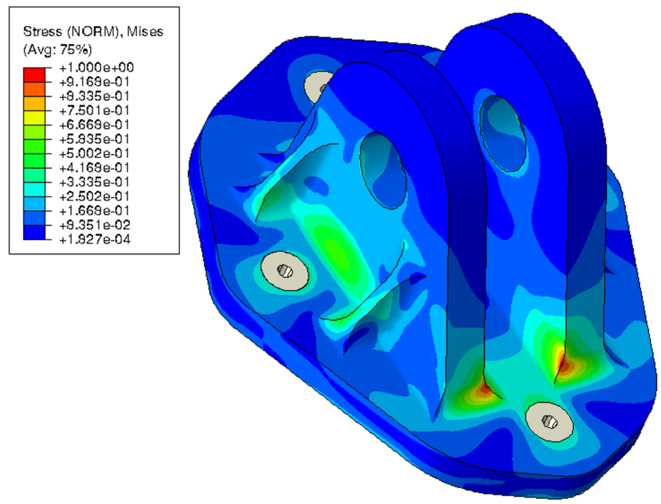

Figure 2. FEM static analysis results of the component made in Al2024-RAM2 (normalized to the maximum peak stress).

Topology optimization and resulting redesign

A topology optimization was performed for this component, although its structural configuration is not ideal for such an approach. The design envelope shown in Figure 3 is severely space constrained due to the surrounding components and the legacy nature of the system, which was originally designed before the introduction of additive manufacturing in this field. The component itself is relatively small and includes several anchoring features and holes whose positions must be fixed and preserved. Accordingly, the regions around these features, highlighted in green in the figure, were excluded from the optimization domain, as their presence is functionally necessary. The aim of this controlled application was not to radically redesign the component, but rather to develop and validate a reliable workflow for DfAM. By first applying the methodology to a well-characterized and validated component within a strictly defined envelope, confidence in the robustness and feasibility of the proposed optimization strategy can

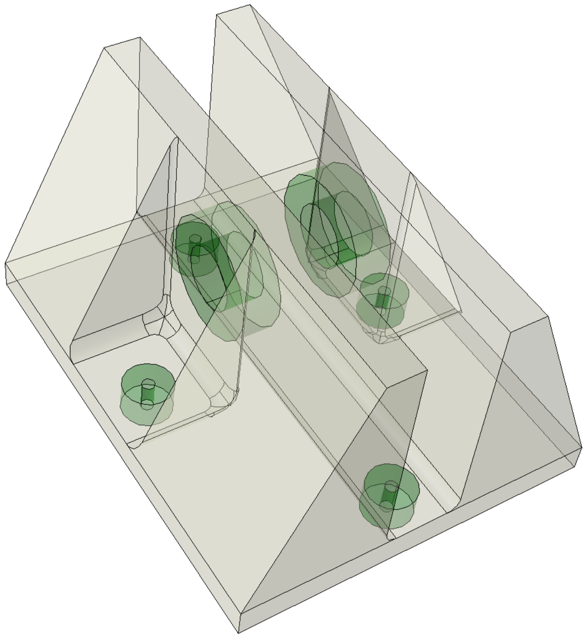

Figure 3. Design envelope defined for the TO. The green regions indicate areas excluded from the optimization domain.

be established before extending it to more complex, less constrained geometries.

The topology optimization was formulated with the objective of minimizing the total strain energy of the component and thus maximizing its stiffness under the specified static loading conditions. Stress constraints were imposed to ensure that the maximum Von Mises equivalent stress remained below the yield strength of the material, which is scaled with a safety factor of approximately 10%. The target volume for the optimized region was set to be less than 20% of the design envelope, except for the non-design areas near the mounting holes, which are subject to strict geometric and functional constraints. The SIMP interpolation method described in the Materials and Methods section was used for the optimization. The optimization was performed with respect to the critical static load case. Subsequently, the optimized design was also evaluated under fatigue conditions to ensure that the stress amplitudes remain below the fatigue limit of the material.

Figure 4 shows the results of one of the test cases performed with the topology optimization approach described above, as obtained from the Abaqus/CAE environment. Since the original component is a mature and well-established design, the topology-optimized shape is, as expected, not significantly different from the initial geometry. Nevertheless, the optimization process identified opportunities for material removal in the regions of the bracket that exhibited lower stress levels in the static analysis (Figure 2). In particular, the removed elements are concentrated in areas that contribute less to the primary structural load path, allowing a reduction in volume without compromising the mechanical integrity of the component. These areas include the upper parts of the lugs above the holes where the tie rod is connected, the outer edges at the base of the bracket and parts of the base section between the two lugs. It can also be observed that the base appears less rounded compared to the original design, indicating a tendency towards a more efficient distribution of material. Furthermore, no material was removed in the vertical lugs region, probably due to the relatively high loading experienced in these areas where any reduction in volume would lead to excessive stress concentrations. Taking into account the need to maintain sufficient space for the attachment of the bracket to the underlying structure through the base holes (using pins and collars), to allow adequate clearance for the insertion of bushings into the lug holes, and the increasing structural importance of the ribs as material is removed, the redesign was refined accordingly to meet these functional and mechanical requirements. This is illustrated in Figure 5, which also shows the convex hull employed in the subsequent printability and optimal build orientation analyses. In the redesigned component, the outermost edges of the base were slightly trimmed and subtly recessed inward as suggested by the topology optimization, while likely maintaining the overall shape dictated by the original geometry. A similar design adjustment was made to the upper areas of the lugs, where material was selectively removed. Furthermore, a hole was inserted at the base between the two lugs, as recommended by the optimization results and supported by the low stress levels observed in this area. The geometry of this hole was carefully defined to avoid sharp internal corners and stress-increasing features that could lead to localized fatigue or failure. At the base of the lugs, in addition to the fillets already present in the original design, further filet features were introduced to make the corners rounder to further smooth the transition between the lugs and the base. This modification has been shown to significantly reduce stress concentrations in these critical areas. The orientations of the base walls, lugs and structural ribs were intentionally left unchanged as these elements were not significantly impacted by the optimization process and play a critical role in maintaining the mechanical integrity and assembly compatibility of the component.

The weight of the bracket was reduced by up to 28.4% compared to the design of the current component made of Al7050 and by 31.3% compared to the original component made of Al2024-RAM2, while still meeting all design requirements. The geometry resulting from the structural optimization is shown in Figure 6, which shows the stress and displacement magnitude fields under the critical static load case. The results are compared directly with those of the original component counterpart, as the same scale is used throughout (scale values omitted). The most significant difference in the stress distribution lies in the location of the maximum stress values: due to the introduction of the hole in the base, the highest stresses in the redesigned component appear near the base of the lugs on the opposite side of the part compared to the original design. However, these stresses are almost identical in magnitude to those observed on the front side of the redesigned component, indicating a balanced and acceptable stress distribution as a result of the geometric changes. Although the displacements may appear slightly increased, they

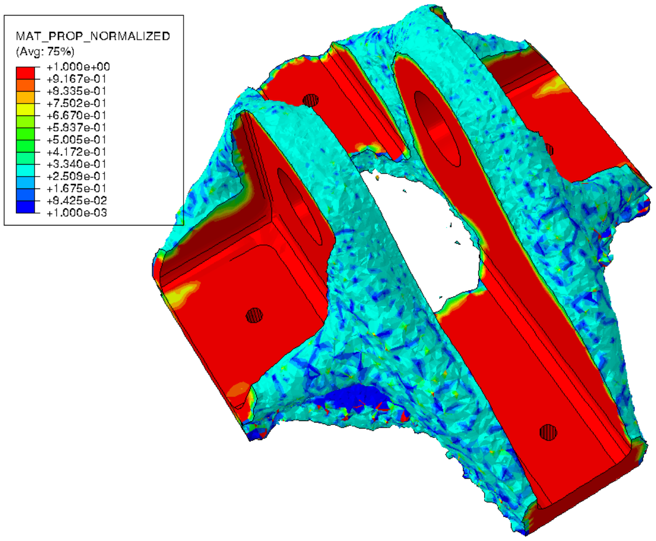

Figure 4. Trial case normalized material property results of TO.

remain in the order of tenths of a millimeter even under the most demanding load cases and are therefore not critical for real-world applications. In addition, the redesigned component was also assessed for fatigue life and no critical issues were found, although safety factors were not explicitly considered.

Printability analysis

Once the component had been redesigned based on the results of the topology optimization, a printability analysis was carried out. The CAD model was exported as a high-quality STL file consisting of 49,890 triangles, a surface quality factor of 0.9597 (defined as the ratio between the number of STL surface faces and the number of triangles) and a relative volume of 0.3595. For the analysis, the material properties, printer specifications, print optimization settings and target function weights required for the *AM-Optimizer* application were used, as described in the Materials and Methods section. For this particular part, the weights assigned to the different elements of the objective function were chosen to reflect both the chosen additive manufacturing technology and the functional requirements of the intended application. As the proposed part design does not have walls classified as thin, the corresponding weight was set to 0%. Similarly, the weight for the maximum build height was set to 0% as this parameter, although directly proportional to the total printing time, is not considered relevant in this case. As this is a functional aerospace part that is still in the design phase and not intended for mass production, the build time is not a critical constraint. In contrast, the weights for the base contact area, support structure requirements, warping risk and surface quality were set at 20%, 30%, 20% and 30% respectively.

The result of the printability analysis and the optimization of the build orientation is shown in Figure 8, which presents the

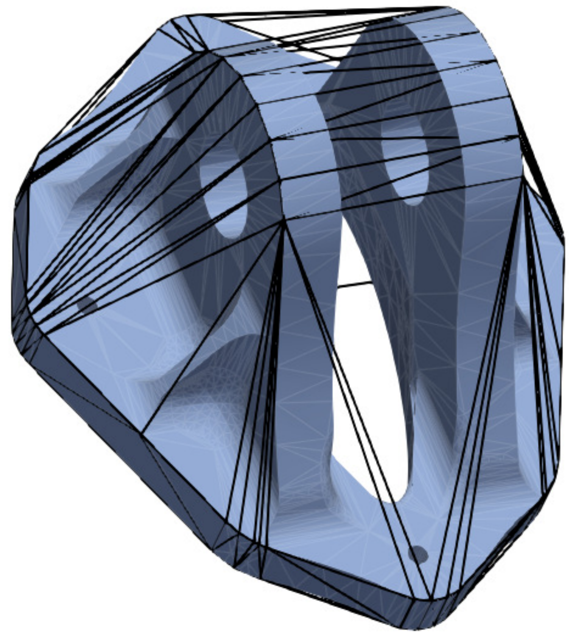

Figure 5. Redesigned bracket geometry following topology optimization, shown together with the corresponding convex hull. The convex hull shown was derived from a low-resolution STL file to improve visual clarity.

results of the tool *AM-Optimizer*. As can be seen in the figure, the application directly outputs the optimal build orientation angle, the corresponding value of the objective function for this orientation, a breakdown of the contributions of each component to this value and the total time required to perform the analysis.

The computation time of approximately 30.3 minutes shown in the figure corresponds to the analysis performed using six CPU cores on a laptop equipped with a 13th Gen Intel® Core™ i7-1370P processor operating at 1.9 GHz, using MATLAB R2024a. Despite the duration, the computation time is reasonable given the high-resolution STL export, the geometric complexity of the part and the fact that the component is a functional, real-world aerospace element. For comparison, if the same analysis is performed with a low-quality export of the component containing only 4,516 triangular elements, the time required is around 16 seconds. As already observed with other additive manufacturing technologies (Ref. 22), this confirms that the tool is capable of processing industrial-scale parts within practical timeframes, even when running on a standard portable computer. This demonstrates that the tool is accessible and practical for a wide range of users. For particularly complex geometries, the number of CPU cores employed during the analysis can be specified by the user before the optimization process begins.

Since the geometry of the component in this case is relatively simple, although not perfectly flat as it may seem at first glance, the optimizer suggests aligning the part so that its base lies directly on the build plate. This suggestion aligns with what a human designer would probably intuitively choose.

prove design decisions accordingly.

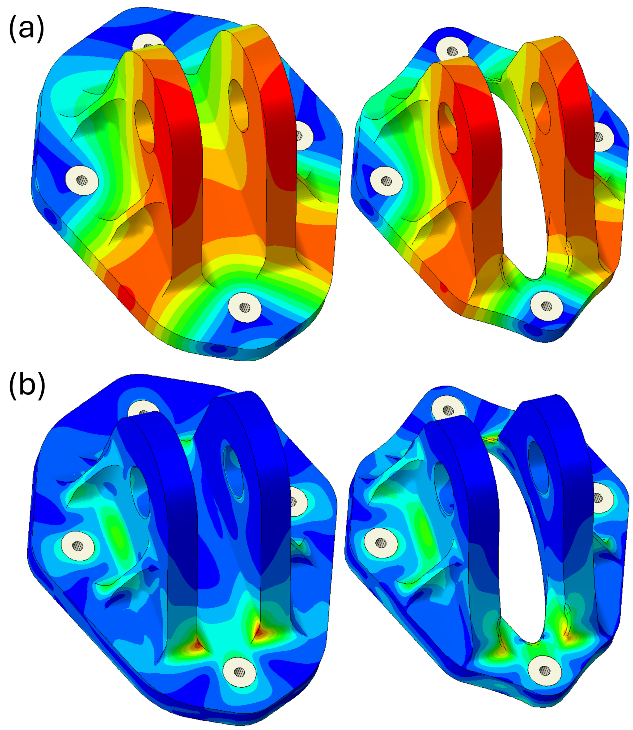

Figure 6. Displacement (a) and Von Mises equivalent stress (b): comparison of the magintude fields of the original and the redesigned bracket under critical static load. The results are uniformly scaled with those of the component with the highest value obtained to allow direct comparison

The result visualization interface allows the user to explore other possible build orientations derived from the convex hull set, arranged in descending order according to the optimization algorithm's evaluation. Within this interface, users can inspect both the overall values of the objective function and the individual component scores for each alternative orientation. Improvements over the optimal solution are highlighted in green, while deteriorations are shown in red. This enables a quick and intuitive comparison of the different build strategies.

This interface also enables the visualization of regions that perform rather poorly with respect to the objective function, i.e. areas that do not reach the minimum acceptability thresholds defined for certain printability criteria. Figure 7 illustrates some of the available display modes: the "Clear" mode, which only shows the orientation of the part on the build platform; the "Supports" mode, which highlights the regions of the component that are likely to need support structures, i.e. in this case the holes on the lugs; and the "Low Quality Surface" mode, which identifies the surface areas that are expected to have insufficient surface quality. In this particular case, these are areas where the surface roughness Ra exceeds the defined limit with values above 7 μm and therefore may require post-processing. These areas are located near the base and top of the lugs, and near the holes on the lugs. These visualization tools help to identify local manufacturability issues and im-

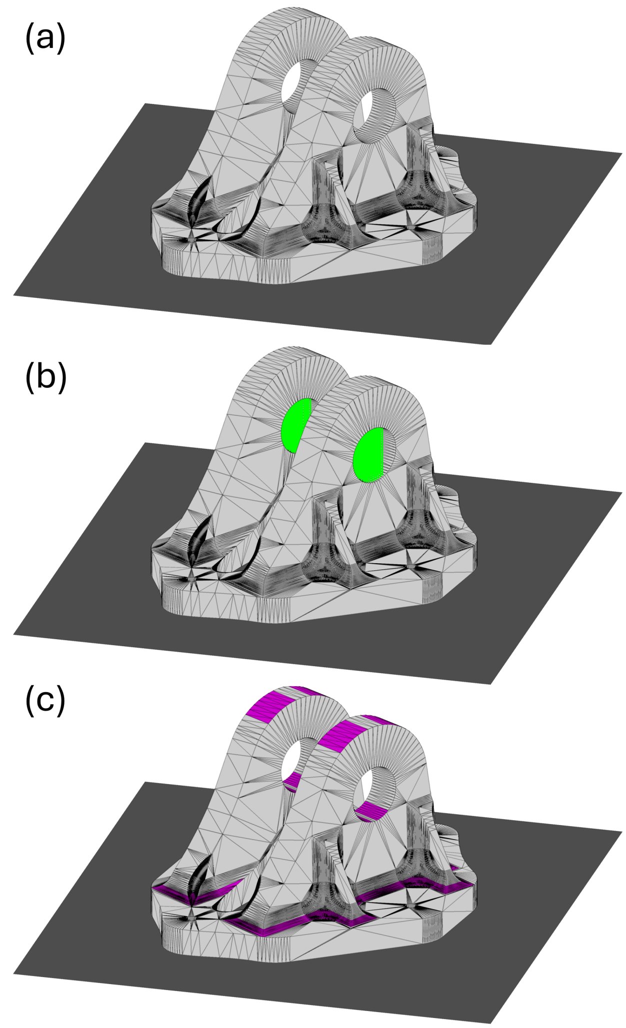

Figure 7. Example of visualization modes available in the *AM-Optimize*r tool: (a) "Clear", (b) "Supports" and (c) "Low quality surface" modes.

In view of the above, it can be concluded that *AM-Optimizer* is a user-friendly application that is accessible even to users without extensive knowledge of additive manufacturing. Thanks to its intuitive user interface, simple setup and customizable parameters, the tool is suitable for quick and effective use on a wide range of components without the need for advanced computational resources. At the same time, the tool proves to be extremely robust and versatile, allowing even more experienced users to fine-tune build orientation optimization and subsequent printability analysis according to specific design requirements. This ensures full transparency and control over the input parameters and output results of the process.

However, it should be noted that the accuracy of the analysis and the resulting evaluation depends heavily on the quality of the STL file used as input, as the tool works directly with

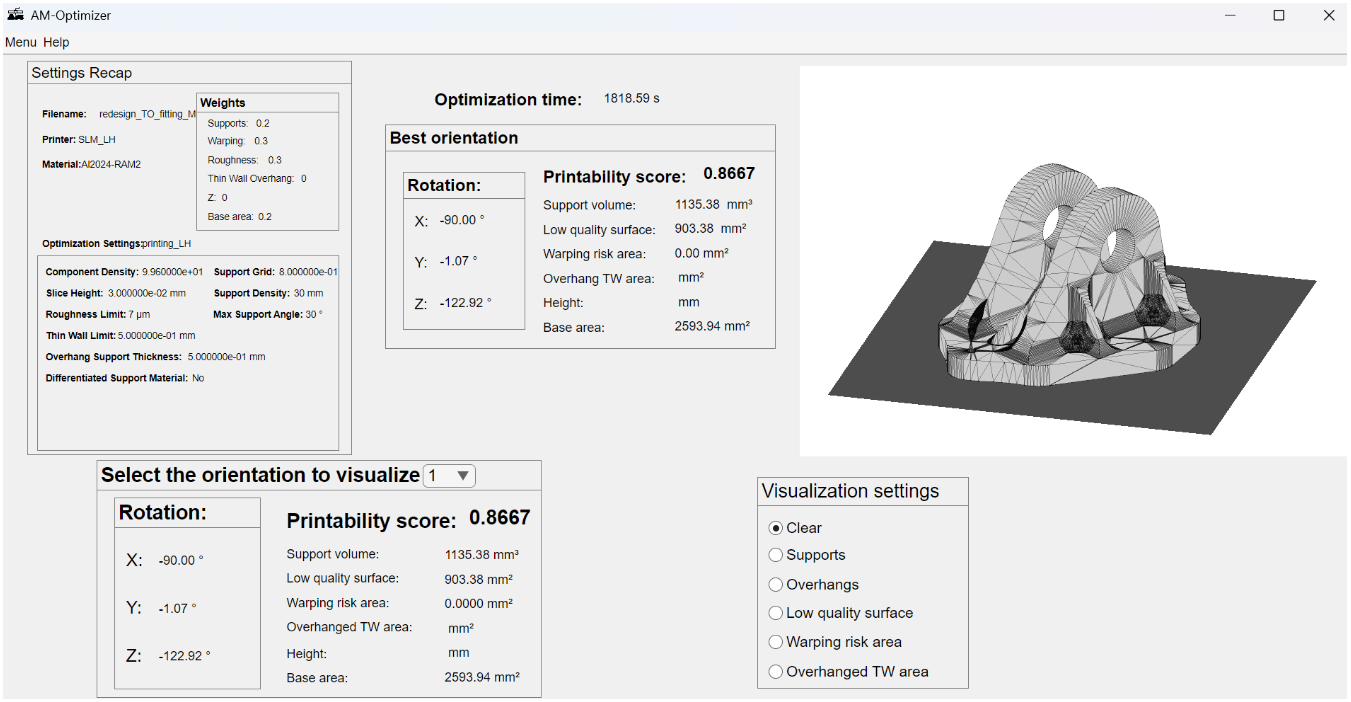

Figure 8. Results of the print orientation optimization performed using the *AM-Optimizer* application.

this geometry. The higher the resolution of the exported STL model, the more detailed and accurate the analysis will be, but at the cost of a higher computing time. The balance between precision and efficiency is therefore at the discretion of the user and depends on the complexity of the part and the specific requirements of the application.

CONCLUSIONS AND FUTURE DEVELOPMENTS

In this study, an established aerospace bracket was analyzed and redesigned to exploit the advantages of additive manufacturing through a comprehensive workflow that combines finite element analysis, topology optimization and printability assessment.

The initial static and fatigue analyzes performed on the original Al2024-RAM2 component confirmed the equivalence of mechanical performance with the base alloy Al7050, with only a slight increase in mass due to the difference in material density. This confirmed the choice of material for the subsequent design changes.

Topology optimization was applied despite the challenging constraints posed by the limited design envelope and fixed anchoring features. The TO results demonstrated that a reduction in component mass of up to 28.4% was possible without compromising structural integrity under both static and fatigue loading. The optimized design effectively removed areas of low stress while maintaining critical load paths, as demonstrated by detailed stress and displacement comparisons.

Subsequently, the redesigned geometry was subjected to a thorough printability analysis using the *AM-Optimizer* application, which made it possible to determine an optimal build orientation that balances support structure requirements, surface quality and warping risk. The tool's intuitive user interface and computational efficiency, achieved even on a standard laptop, underline its practical suitability for industrial applications, but even for users without extensive AM knowledge.

Overall, the proposed methodology provides a robust and accessible approach to design for additive manufacturing that integrates structural optimization and manufacturability assessment to deliver lightweight, reliable and manufacturable components. Future work will primarily focus on extending this workflow to more complex and fully functional aerospace components to move beyond demonstrating the applicability of the methodology to its practical implementation in the design of functional parts. Furthermore, the integration of printability and build orientation analysis directly into the optimization process is envisaged to enable truly printability-driven design for additive manufacturing from the earliest stages of component development.

Author contact: Bianca Omede' bianca.omede@polimi.it, Simone Festa simone.festa@mail.polimi.it, Maurizio Tirelli maurizio.tirelli@leonardo.com, Gabriele Fantoni gabriele.fantoni@leomardo.com, Sergio Sartori sergio.sartori@leonardo.com, Antonio Mattia Grande antoniomattia.grande@polimi.it

ACKNOWLEDGMENTS

Funded by the European Union – Next Generation EU, Mission 4 Component 1, CUP D43C23002190008. The authors would like to thank Tiziana Biasutti and Giovanni Agostoni for their valuable support in retrieving the material and printing data.

REFERENCES

1. Ian Gibson, David Rosen, and Brent Stucker. *Additive manufacturing technologies: 3D printing, rapid prototyping, and direct digital manufacturing, second edition*. Springer New York, 1 2015.
2. Paul F. Egan. Design for additive manufacturing: Recent innovations and future directions. *Designs*, 7, 8 2023.
3. Mary Kathryn Thompson, Giovanni Moroni, Tom Vaneker, Georges Fadel, R. Ian Campbell, Ian Gibson, Alain Bernard, Joachim Schulz, Patricia Graf, Bhrigu Ahuja, and Filomeno Martina. Design for additive manufacturing: Trends, opportunities, considerations, and constraints. *CIRP Annals - Manufacturing Technology*, 65:737–760, 2016.
4. Abdullah Alfaify, Mustafa Saleh, Fawaz M. Abdullah, and Abdulrahman M. Al-Ahmari. Design for additive manufacturing: A systematic review. *Sustainability (Switzerland)*, 12, 10 2020.
5. Sheng Yang and Yaoyao Fiona Zhao. Additive manufacturing-enabled design theory and methodology: a critical review. *International Journal of Advanced Manufacturing Technology*, 80:327–342, 9 2015.
6. Narjess Chtioui, Raoudha Gaha, and Abdelmajid Benamara. Design for additive manufacturing: Review and framework proposal, 2 2023.
7. Anton Wiberg, Johan Persson, and Johan Ölvander. Design for additive manufacturing – a review of available design methods and software. *Rapid Prototyping Journal*, 25:1080–1094, 8 2019.
8. Byron Blakey-Milner, Paul Gradl, Glen Snedden, Michael Brooks, Jean Pitot, Elena Lopez, Martin Leary, Filippo Berto, and Anton du Plessis. Metal additive manufacturing in aerospace: A review. *Materials and Design*, 209, 11 2021.
9. Lorenzo Alari, Sergio Sartori, Paolo Pisani, Federico Montagna, Nicola Borlin, and Diego Scaltritti. Helicopter drive system featuring additive-manufactured components. In *Lecture Notes in Networks and Systems*, volume 1124 LNNS, pages 75–83. Springer Science and Business Media Deutschland GmbH, 2024.
10. Airbus Helicopters. Airbus helicopters boosts competitiveness with 3d printing, 2023. https://www.airbus.com/en/newsroom/press-releases/2023-10-airbus-helicopters-boosts-\competitiveness-with-3d-printing, accessed June 19, 2025.
11. Roberto Montanari, Alessandra Palombi, Maria Richetta, and Alessandra Varone. Additive manufacturing of aluminum alloys for aeronautic applications: Advantages and problems. *Metals*, 13, 4 2023.
12. Lidong Wang, Reed Mosher, and Patti Duett. Additive manufacturing in the aerospace industry. *American Journal of Engineering and Applied Sciences*, 17:116–125, 3 2024.
13. Martin P. Bendsøe and Ole Sigmund. *Topology Optimization: Theory, Methods, and Applications*. Springer Berlin, Heidelberg, 2 edition, 2004.
14. S. Satya Hanush and M. Manjaiah. Topology optimization of aerospace part to enhance the performance by additive manufacturing process. *Materials Today: Proceedings*, 62:7373–7378, 1 2022.
15. Jinlong Su, Yang Mo, Peijie Shangguan, Chinnapat Panwisawas, Fulin Jiang, and Swee Leong Sing. Additive manufacturing-by-design for support structures: a critical review. *International Journal of Extreme Manufacturing*, 7, 10 2025.
16. R. J. Ferreira, A. M. Grande, J. M. Guedes, A. M. Deus, and G. Sala. Combination of topology and shape optimization with finite element modeling in the case of an aerospace component produced by laser based additive manufacturing. *Journal of Laser Applications*, 35, 5 2023.
17. Miguel Seabra, José Azevedo, Aurélio Araújo, Luís Reis, Elodie Pinto, Nuno Alves, Rui Santos, and João Pedro Mortágua. Selective laser melting (slm) and topology optimization for lighter aerospace componentes. In *Procedia Structural Integrity*, volume 1, pages 289–296. Elsevier B.V., 2016.
18. Marijn P. Zwier and Wessel W. Wits. Design for additive manufacturing: Automated build orientation selection and optimization. In *Procedia CIRP*, volume 55, pages 128–133. Elsevier B.V., 2016.
19. Lin Cheng and Albert To. Part-scale build orientation optimization for minimizing residual stress and support volume for metal additive manufacturing: Theory and experimental validation. *Computer-Aided Design*, 113:1–23, 2019.
20. Hannah D. Budinoff and Sara McMains. Will it print: a manufacturability toolbox for 3d printing. *International Journal on Interactive Design and Manufacturing*, 15:613–630, 12 2021.
21. Hongsheng Sheng, Jinghua Xu, Shuyou Zhang, and Jianrong Tan. Build orientation optimization for extrusion-based additive manufacturing coupling with adaptive slicing. *International Journal of Advanced Manufacturing Technology*, 123:1133–1158, 11 2022.
22. Simone Festa. Am-optimizer: Developing an application to detect critical areas and drive printing orientation in additive manufacturing. Master's thesis, Politecnico di Milano, 2025.
23. G I N Rozvany, M Zhou, and T Birker. Structur optimitation generalized shape optimization without homogenization*. *Structural Optimization*, 4:250–252, 1992.
24. Radomila Konecna, Tibor Varmus, Gianni Nicoletto, and Michal Jambor. Influence of build orientation on surface roughness and fatigue life of the al2024-ram2 alloy produced by laser powder bed fusion (l-pbf). *Metals*, 13, 9 2023.

25. Seren Senol, Guichuan Li, Vivek Devulapalli, Etienne Brodu, and Kim Vanmeensel. High strength and fatigue performance achieved for l-pbf processed hybrid particle reinforced al-cu-mg composite. *Composites Part B: Engineering*, 285, 10 2024.

26. elementum3D. A2024-ram2 material data sheet. Technical report, Elementum 3D, August 2023.

27. Tibor Varmus, Radomila Konecna, Gianni Nicoletto, and Federico Uriati. Microstructure and fatigue properties of al2024-ram2 aluminum alloy obtained by laser powder bed fusion. In *Procedia Structural Integrity*, volume 43, pages 184–189. Elsevier B.V., 2023.